

# **NOx Control Options and Integration for US Coal Fired Boilers**

## **Quarterly Progress Report**

Reporting Period Start Date: April 1, 2001  
Reporting Period End Date: June 30, 2001

Mike Bockelie, REI  
Marc Cremer, REI  
Kevin Davis, REI  
Bob Hurt, Brown University  
Eric Eddings, University of Utah

July 27, 2001

DOE Cooperative Agreement No: DE-FC26-00NT40753

Reaction Engineering International  
77 West 200 South, Suite 210  
Salt Lake City, UT 84101

## **Disclaimer**

“This report was prepared as an account of work sponsored by an agency of the United States Government. Neither the United States Government nor any agency thereof, nor any of their employees, makes any warranty, express or implied, or assumes any legal liability or responsibility for the accuracy, completeness, or usefulness of any information, apparatus, product, or process disclosed, or represents that its use would not infringe privately owned rights. Reference herein to any specific commercial product, process, or service by trade name, trademark, manufacturer, or otherwise does not necessarily constitute or imply its endorsement, recommendation, or favoring by the United States Government or any agency thereof. The views and opinions of authors expressed herein do not necessarily state or reflect those of the United States Government or any agency thereof.”

## Abstract

This is the third Quarterly Technical Report for DOE Cooperative Agreement No: DE-FC26-00NT40753. The goal of the project is to develop cost effective analysis tools and techniques for demonstrating and evaluating low NO<sub>x</sub> control strategies and their possible impact on boiler performance for firing US coals. The Electric Power Research Institute (EPRI) is providing co-funding for this program. This program contains multiple tasks and good progress is being made on all fronts. A Rich Reagent Injection (RRI) design has been developed for a cyclone fired utility boiler in which a field test of RRI will be performed later this year. Initial evaluations of RRI for PC fired boilers have been performed. Calibration tests have been developed for a corrosion probe to monitor waterwall wastage. Preliminary tests have been performed for a soot model within a boiler simulation program. Shakedown tests have been completed for test equipment and procedures that will be used to measure soot generation in a pilot scale test furnace. In addition, an initial set of controlled experiments for ammonia adsorption onto fly ash in the presence of sulfur have been performed that indicates the sulfur does enhance ammonia uptake.

## Table of Contents

DISCLAIMER.....	i
ABSTRACT.....	ii
TABLE OF CONTENTS.....	iii
EXECUTIVE SUMMARY .....	1
EXPERIMENTAL METHODS.....	2
Task 1 Program Management .....	2
Task 2 NO <sub>x</sub> Control.....	2
Task 3 Minimization of Impacts.....	7
Task 4 SCR Catalyst Testing.....	16
Task 5 Fly Ash.....	17
Task 6 Field Validation of Integrated Systems.....	22
RESULTS AND DISCUSSION .....	22
CONCLUSIONS .....	23
LITERATURE REFERENCES .....	24

## Executive Summary

The work to be conducted in this project received funding from the Department of Energy under Cooperative Agreement No: DE-FC26-00NT40753. This project has a period of performance that started February 14, 2000 and continues through February 13, 2002.

Our program contains five major technical tasks:

- evaluation of Rich Reagent Injection (RRI) for in-furnace NO<sub>x</sub> control
- demonstration of RRI technologies in utility boiler scale field tests
- impacts of combustion modifications (including corrosion and soot)
- ammonia adsorption / removal from fly ash
- SCR catalyst testing

To date good progress is being made on the overall program. We have seen considerable interest from industry in the program due to our initial successful field tests of the RRI technology and the corrosion monitor.

During the last three months, our accomplishments include the following:

- To study the applicability of using RRI for PC fired boilers, a single burner modeling study has been performed for in-burner reagent injection. Model results indicate NO<sub>x</sub> reductions of up to 20% can be obtained. Potentially greater NO<sub>x</sub> reductions can be obtained by layering in-burn injection with other furnace injection strategies.
- Bench and pilot scale tests are being conducted to calibrate a corrosion probe to monitor water wall wastage. A field test of the corrosion probe is scheduled for next quarter.
- Comparisons between model predictions and experimental measurements of soot generation for low NO<sub>x</sub> firing conditions have demonstrated qualitative agreement. Further work on both the model and the experimental methods will be required to obtain quantitative agreement.
- A contract modification has been received from DOE that will provide additional funds for an in-scope change to our work plan for investigating SCR catalysts. The modified work plan allows investigating the impact of biomass co-firing on SCR catalyst performance and includes Prof. Larry Baxter (Brigham Young University) in the program.
- A first set of fundamental ammonia isotherms was measured on commercial carbon-containing fly ash samples and compared to similar data for nitrogen and carbon dioxide to understand the fundamental nature of ammonia adsorption. The governing mechanism shifts from mineral adsorption to combined physical/chemical adsorption on carbon as the gas phase ammonia concentration increases. Uptake in simulated flue gas is higher than in pure ammonia, likely due to synergistic effects of one of the secondary species, which will be the subject of future experiments.

## Experimental Methods

Within this section we present in order, brief discussions on the different tasks that are contained within this program. For simplicity, the discussion items are presented in the order of the Tasks as outlined in our original proposal.

### Task 1 - Program Management

A contract modification has been authorized by DOE that will provide additional funds for an in-scope change to our work plan for investigating SCR catalysts. The modified work plan allows investigating the impact of biomass co-firing on SCR catalyst performance and provides funding to include Prof. Larry Baxter (Brigham Young University) in the program.

#### Industry Involvement

On June 21, 2001, REI met with Dave O'Connor (EPRI Project Manager, Combustion Performance), to provide a brief update on the status of our project, with a particular emphasis on the modeling efforts for Rich Reagent Injection (RRI).

### Task 2 - NOx Control – LNFS/SNCR/Reburning

#### Task 2.3 Evaluation of Rich Reagent Injection for PC Furnace Applications

As part of investigating the application of Rich Reagent Injection (RRI) in PC furnaces, model evaluations have been completed to investigate the NOx reduction performance of injection of aqueous urea into the burner zone of a PC wall-fired furnace. In the last quarterly report, a discussion was given of PC furnace calculations involving the injection of aqueous urea into the lower furnace of staged PC furnaces. In those calculations, both wall and in-burner injection strategies were investigated. During this quarter, the strategy of in-burner injection was investigated in greater depth through a single burner model of the process.

#### Details of Research and Methodology

The burner design that was investigated was that of a conventional wall burner that was modified through the addition of a flame stabilizer that creates an internal fuel rich recirculation zone. Reagent injection into and around the region of the internal recirculation zone (IRZ) was investigated through CFD modeling. Analyses were carried out using two approaches: 1) chemical kinetic calculations along streamlines, 2) CFD calculations incorporating reduced chemistry. The streamline calculations were performed to utilize previously completed CFD predictions. The predicted flow field, gas temperature, and distributions of the major species were used to provide inputs to detailed chemical kinetics calculations of reagent injection along streamlines. The second approach was to perform new CFD model calculations using REI's proprietary models, which couple the calculation of the flow field with the reagent injection chemistry.

## Streamline Analysis

Two-dimensional, axi-symmetric CFD combustion simulations were previously performed for a wall burner incorporating low NO<sub>x</sub> modifications. Burner stoichiometric ratios of 1.03 (unstaged) and 0.83 (staged) were considered. Based on the results of these combustion simulations, a streamline analysis was performed by REI to examine the potential benefit of in-burner rich reagent injection. Four streamlines were tracked from the burner through the combustion field.

In all streamline simulations, it was assumed that the urea reagent was released into the gas phase within the burner primary air zone (this is only an assumption for the streamline calculations). The predicted temperature, and major species history along these streamlines were used within Chemkin calculations, assuming an initial NO<sub>x</sub> concentration and a specified initial normalized stoichiometric ratio (NSR) for urea reagent (urea was assumed to split into 50% NH<sub>3</sub> and 50% HNCO).

For the streamline analysis, an initial NO<sub>x</sub> concentration of 400 ppm and an initial NSR of 2 were chosen for the Chemkin calculations. The predicted NO<sub>x</sub> reduction and NH<sub>3</sub> slip at the end of the streamline calculations, due to the addition of reagent, are plotted in Figure 2.1 for both unstaged and staged cases.

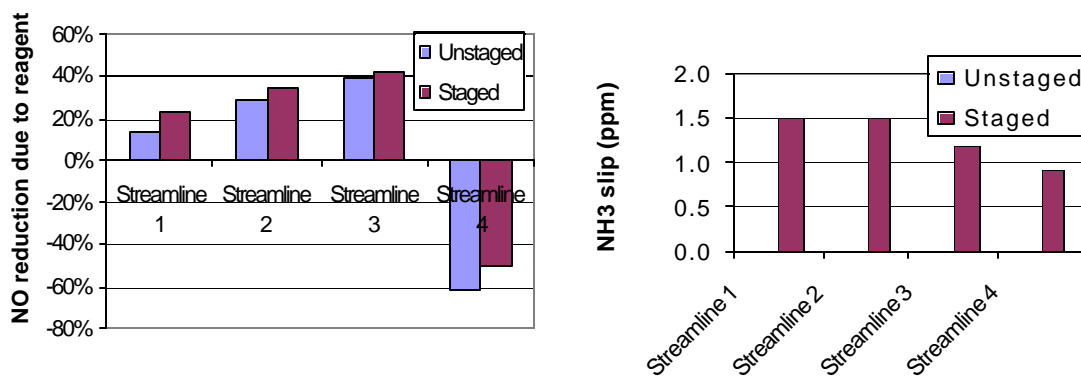


Figure 2.1: Predicted NO<sub>x</sub> reduction and NH<sub>3</sub> slip of streamline calculations for an initial NO<sub>x</sub> of 400 ppm and initial NSR of 2.0.

NO<sub>x</sub> reduction for the streamlines 1-3 and NO<sub>x</sub> increase for the streamline 4 due to the reagent were observed for both the staged and unstaged cases. Negligible NH<sub>3</sub> slip was predicted for both cases. Even though the predicted NO<sub>x</sub> reduction along the streamlines for the staged case was better than corresponding streamlines for the unstaged case, one would expect even better performance. Review of staged and unstaged cases show that the predicted temperature and equivalence ratio for the staged case are more suitable for RRI than in the unstaged case. Upon examination of the reagent consumption history, it was found that much of the reagent is consumed in the first 0.3 seconds residence time which corresponds to ¼ of the length of the burner model. Thus, an increase of the initial NSR of the streamlines may provide quite different results.

In practice, the amount of reagent injected through the burner is determined by the total NO<sub>x</sub> flow rate and a chosen overall NSR. We have typically found that an overall NSR of 2.0 is nearly optimal. The streamline calculations in Figure 1 also provide an estimation of the treatable flow region for reagent injection. The inner envelope defined by streamline 4 can be considered the treatable region, since outside of that envelope reagent is oxidized and NO<sub>x</sub> is increased rather than reduced. The NSR for the streamlines in the treatable flow should be calculated through the overall NSR and the mass fraction of the treatable flow. The treatable flow mass fraction for the unstaged case was calculated to be approximately 12.7%. Additional calculations for the staged case showed that the treatable region could be extended and the mass fraction of this treatable flow was about 29.7%. Recalculation along the streamlines using the adjusted NSRs for both the staged and unstaged cases produced the results shown in Figure 2. For the staged case, the fuel rich and optimal temperature (1500K-2050K) region was fully utilized to reduce NO<sub>x</sub> to close to 0 ppm. However, NH<sub>3</sub> slip for these streamlines is significant as shown in Figure 2.2.

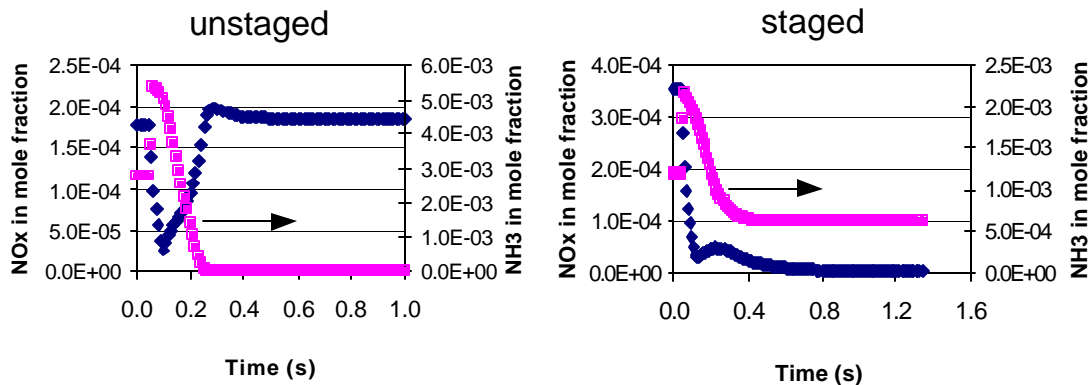


Figure 2.2. The NO<sub>x</sub> and NH<sub>3</sub> concentration as a function of residence time for streamline 3 for both staged and unstaged cases.

Several conclusions can be drawn from the streamline analysis. The small mass fraction of treatable flow for the unstaged case and the predicted poor NO<sub>x</sub> reduction due to reagent injection in the streamline calculations make the application of rich reagent injection in the unstaged operation very problematic. For the staged case, the streamline analysis indicates that approximately 30% of the mass flow is treatable. Combining this with reasonable NO<sub>x</sub> reduction in this region indicates that possible 15-20% reduction in NO<sub>x</sub> due to in burner reagent injection may be expected.

### CFD Analysis

Simulations of the low-NO<sub>x</sub> burner modifications were also performed using REI's proprietary CFD software *Glacier*. These simulations allowed us to couple the combustion calculations with the rich reagent injection chemistry calculations rather than carrying out streamline calculations as was discussed above. The same single burner model geometry that was used in the axisymmetric calculations was used for the *Glacier* simulations. Simulations focused on staged operation since it has the greatest potential for significant NO<sub>x</sub> reduction with RRI.



The first baseline simulation was performed without in-burner urea reagent injection. The predicted center plane temperature and O<sub>2</sub> distributions are shown in Figures 2.3 and 2.4, respectively. Coal burnout and NO<sub>x</sub> emissions were predicted to be 82% and 305 ppm, wet. These values are consistent with the level of staging. However, the predicted temperature distribution in Figure 2.3 is significantly different from that predicted in the axi-symmetric case. An important difference is the predicted temperature in the fuel rich core of the internal recirculation zone which Glacier predicts to be significantly lower.

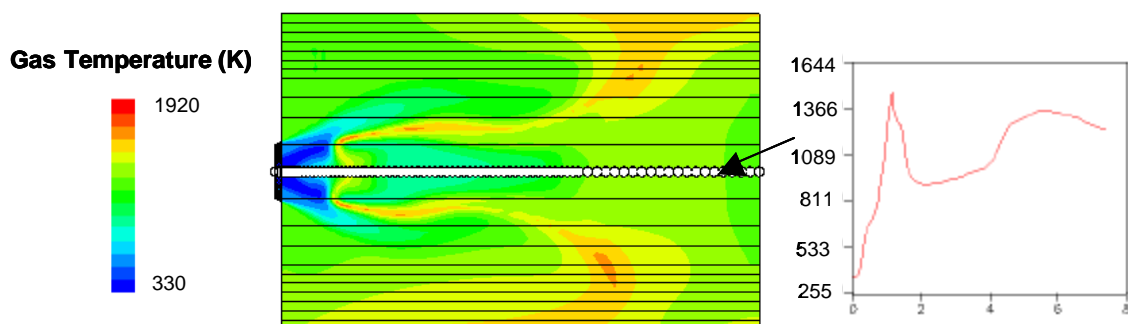


Figure 2.3. Predicted temperature distribution at the center plane of low-NO<sub>x</sub> burner simulation.

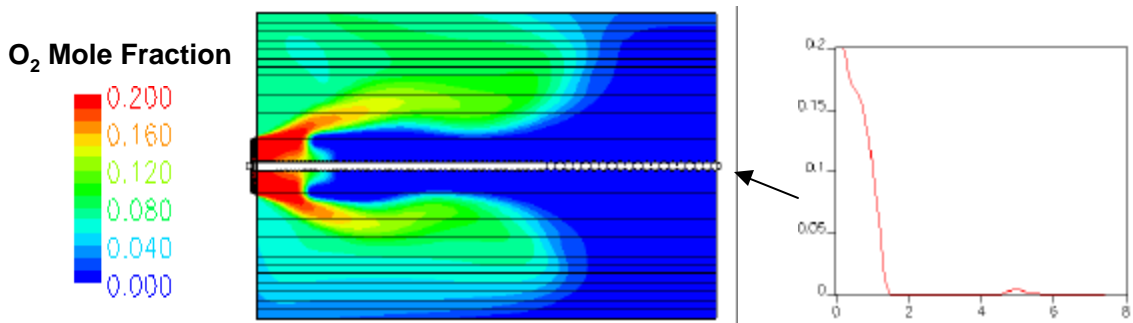


Figure 2.4. Predicted O<sub>2</sub> distribution at the center plane of low-NO<sub>x</sub> burner simulation.

Four RRI cases were considered. In all four cases, gas phase urea products (NH<sub>3</sub> and HNCO) were assumed to be released at a specified location in the model (urea seeding). This is in contrast to actual simulation of the aqueous urea injection process. The reason for this modeling strategy was to remove the uncertainty regarding location of actual urea release. The urea seeding locations for the four cases are shown in Figure 2.5. The overall NSR was chosen to be 2.0 in all cases, based on the predicted model exit NO<sub>x</sub> for the baseline case (305 ppm, wet). In case 1, urea was uniformly seeded within the burner primary zone. In case 2, the urea was seeded within the internal re-circulation zone. In case 3, the urea was seeded immediately downstream of the internal re-circulation zone. In case 4, the urea was uniformly seeded at the plane  $\frac{3}{4}$  of the model length (in the post flame gases). The predicted NO<sub>x</sub> reduction and NH<sub>3</sub> slip for baseline case and the four urea seeding cases are given in the Table 2.1.

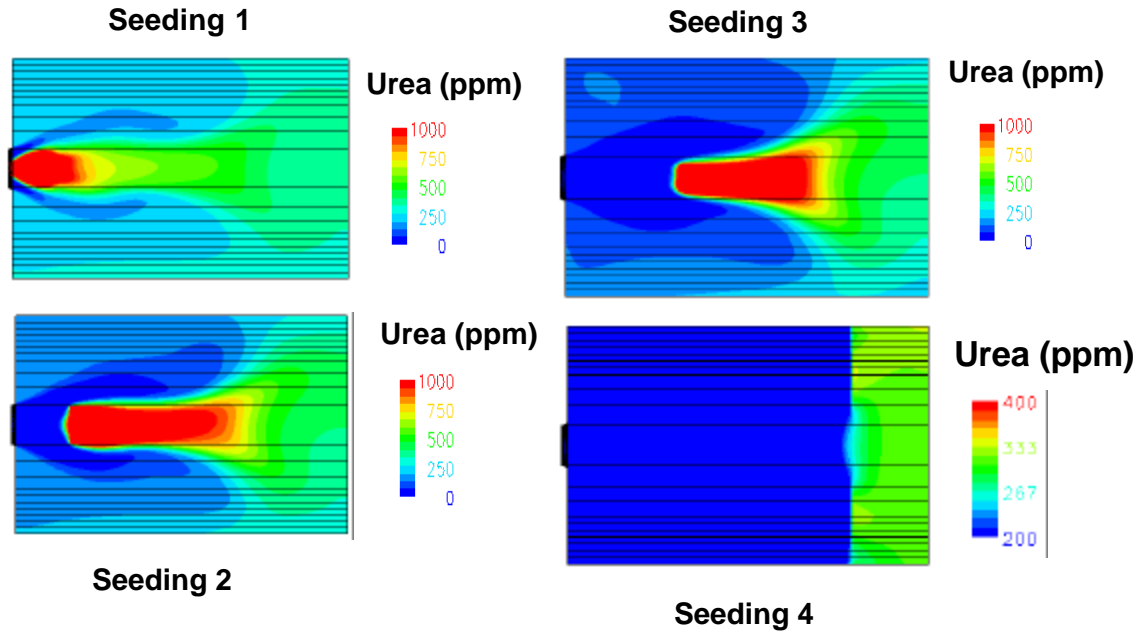


Figure 2.5. Predicted distribution of gas phase urea products based on the initial seeding locations for the four low-NO<sub>x</sub> burner simulated cases.

Table 2.1 NO<sub>x</sub> emission and NH<sub>3</sub> slip for the urea seeding cases

	Base Case	Seeding1	Seeding2	Seeding3	Seeding4
NO <sub>x</sub> (wet, ppm)	305	274	249	246	280
NO <sub>x</sub> Reduction	N/A	10.2%	18.4%	19.3%	8.2%
NH <sub>3</sub> slip (ppm)	2	3.6	9	15	28

For case 1, the majority of the reagent was consumed in the reaction zone of the flame. NO<sub>x</sub> reduction was predicted to be approximately 10%. The NO<sub>x</sub> reduction for seeding case 2 was predicted to increase to 18% with a corresponding increase in NH<sub>3</sub> slip to 9 ppm. Although this burner model predicts excess NH<sub>3</sub> at the exit, this does not translate to NH<sub>3</sub> slip from the furnace since additional residence time under fuel lean conditions will consume most if not all of the remaining NH<sub>3</sub>. Seeding immediately after the internal re-circulation zone in case 3 helped to increase the NO<sub>x</sub> reduction to 19% with an increase in NH<sub>3</sub> slip to 15 ppm. Uniform distribution of urea in the whole plane at about ¾ length of the model length did not work well since reagent at the high temperature fuel lean region formed additional NO<sub>x</sub>.

## Task 3 – Minimization of Impacts

### Task 3.1 Waterwall Wastage

Work on the corrosion probe has been focused on three areas: 1) calibration and verification of probe results, 2) design and construction of an updated corrosion monitoring system, 3) preparation for Eastlake Station field test.

#### *Calibration and Verification*

**Bench-scale Tests:** A test circuit has been developed to check the response of the Electrochemical Impedance (EIM) and Electrochemical Noise (EN) modules. This “test box” determines if the EN and EIM modules are out of calibration by directly measuring their response to a specific signal. If the modules are out of calibration, electronic settings may be modified. Bench-scale tests are underway and should be completed within the next quarter. More tests, covering a variety of simulated conditions, are needed for an accurate calibration. The experimental setup and procedures developed last quarter still holds with few additions. In order to eliminate the flow of corrosive gases through the sensor array (a problem unique to the lab setup due to the lower heat flux) a few changes in our procedure have been implemented:

- Improving the seal between the end-cap and sensor array to minimize leakage through the probe face.
- Maximizing compression between ceramic spacers and steel sensor plates to eliminate leakage through the array and improve conductivity.
- The diameters of the thermo-wells in the temperature sensor plate were increased to ensure the correct depth of the thermocouples during repeated removal and reinsertion required in the lab testing. This depth is critical in calculating the correct temperature at the probe face.

**Pilot-scale Tests:** In order to prepare for full-scale plant tests, the corrosion monitoring system was moved from the laboratory to the large (5 MMBtu/hr) pilot-scale test facility at the University of Utah, known as the L1500. The L1500 is equipped with burners for firing either coal or natural gas. While firing natural gas, the probe was exposed to “clean” operating conditions that served as a baseline for the coal combustion tests. During the coal combustion tests, which used Illinois No. 5 coal due to its high sulfur content, the gas sweeping past the face of the probe was laden with ash particles and operating conditions were varied from sub-stoichiometric firing to fuel-lean operation. The probe was inserted into the furnace near the flame zone and about one foot upstream of the overfire air injection port. The combustion temperatures at the probe face were comparable to actual operation (~3000°F) and the sensor array was cooled to maintain a waterwall temperature of ~850°F.

When the corrosion probe was moved into the furnace, several modifications were necessary. These included the installation of a cooling water circuit to allow the probe to cope with the high heat flux, changing electronics, and rechecking for leaks in the probe sensor head. Several days were spent correcting and, more importantly, documenting the necessary changes to make the probe operate effectively. Figure 3.1 shows the response of the corrosion sensor to changes in stoichiometric ratio (S.R.). It is noted that the maxima in S.R. which represent lean burn conditions correspond to low corrosion rates. Also, the minima in S.R., which represent reducing conditions, show high corrosion rates.

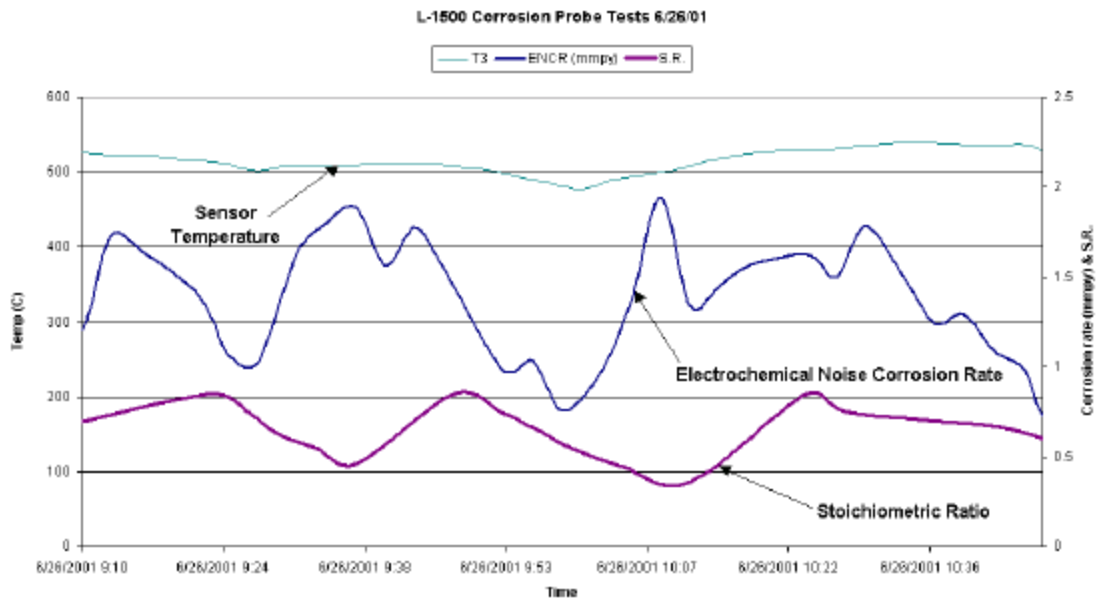


Figure 3.1 Effect of stoichiometric ratio on corrosion rate.

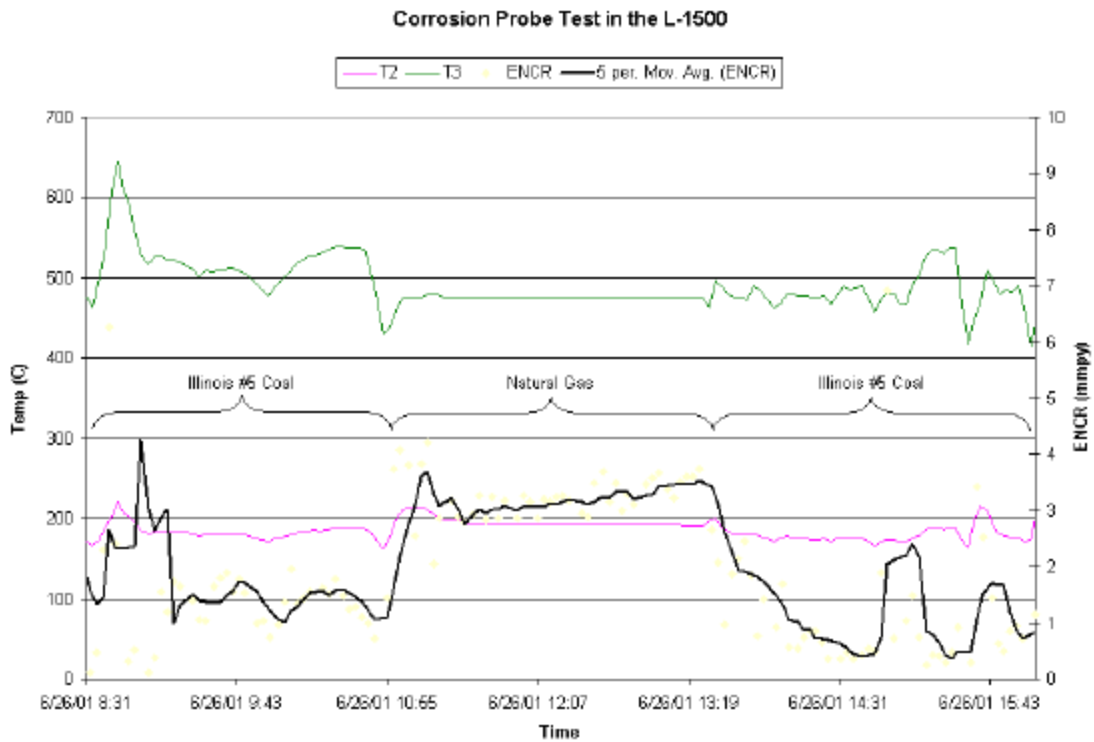


Figure 3.2 Electrochemical noise corrosion rate results from L1500 pilot-scale tests.

Figure 3.2 is an example of the corrosion results measured during one day of the high sulfur coal and natural gas testing in the L1500. The probe was exposed to a variety of furnace operating

conditions ranging from stoichiometric ratios of 0.45 to 1.10. During this time period, the average corrosion rate was measured at about 2 mm/year. By comparison, the results of the profilometry, over the entire test week, showed a corrosion rate of 0.6 mm/yr. Preliminary investigations indicate that two possible sources of this discrepancy are: (i) large excursions in non-uniform corrosion due to unsteady conditions and (ii) non-discrimination of below-threshold ZRA signal.

The corrosion rate data from the probe is integrated to obtain total corrosion depth over the test duration. Any large excursions in corrosion rate over a short duration of time would affect the overall result in the integration of the corrosion depth. In the tests in L1500, it was found that such excursions occurred when the furnace run out of coal and meaningful corrosion rates were restored once combustion was re-established. However fundamental assumptions in the use of this technology require that the corrosion phenomena be relatively steady and the changes that can occur at lab/pilot scale such as SR fluctuations from extremely rich to extremely lean can violate these assumptions

The electrochemical noise corrosion rate is measured from the fluctuations in current (ZRA) and potential as a consequence of corrosion at the exposed metal surface. The fluctuations in potential are referred to as potential noise (EPN) and those in the current as current noise (ECN). From these two values, the resistance noise (ERN) is calculated as

$$\text{ERN} = \frac{\text{EPN}}{\text{ECN}}$$

The corrosion current is computed as

$$I_{\text{CORR}} = \frac{\text{SG}}{\text{ERN}}$$

Where SG is the Stern-Geary constant.

Finally the corrosion rate (ENCR) is calculated as a product of material constant (MC) and the corrosion current as

$$\text{ENCR} = \text{MC} \times I_{\text{CORR}}$$

It may be noted that for insignificant corrosion, the ZRA will be very low. There exists a cut-off value of ZRA below which the current noise ceases to represent meaningful corrosion phenomena. If values of ZRA below the threshold are used in the computation, the integrated corrosion depth will be overestimated. Currently, we are working on incorporation of a feature in the software to identify the below-threshold ZRA values, such as occurred during the period in Figure 3.2 identified as relating to natural gas firing.

## Design and Fabrication

In preparation for the Ohio Coal Development Office (OCDO) field test in mid-July, a new corrosion monitor box and probe body was fabricated. Figure 3.3 shows the new electronics for the system.

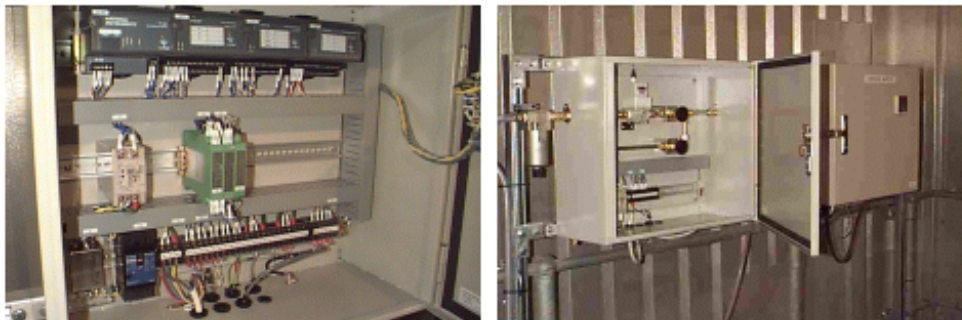


Figure 3.3 New Electronic System Design Including DIN Rail Mounting

Key features of the new probe design include:

1. Easy access to sensor array by means of a shorter end cap and different bolt configuration
2. Quick-connections for air and probe cable
3. All connections are made off the back end, i.e. no connections off the side
4. Attachment pieces to extend the length of probe to accommodate deeper ports
5. Sensor configuration did not change
6. New sensor plates and ceramic spacers

The corrosion monitoring box has been completely redesigned keeping only the fundamentals the same. Updates include:

1. Rack-mounting in dust/water-proof steel cabinets
2. A laptop computer is used for data acquisition to facilitate size and convenience
3. National Instrument DIN rail modules are used to interface components and generate current output
4. The EN and EIM modules were redesigned to accommodate DIN rail mounting as opposed to A/D boards
5. The EN and EIM modules have a larger signal range than the older models, so in normal situations the gain does not have to be altered
6. The manner in which the corrosion rate is calculated has been changed to incorporate the effect of below-threshold ZRA
7. The new system can accommodate up to three probes running simultaneously
8. The cable connecting the probe and the corrosion monitoring box is enclosed in seal-tight to prevent damage and noise
9. The large air control valve has been replaced by a smaller valve.

## FirstEnergy Eastlake Station Field Test

The viewport door from the boiler at which the field test will be performed has been modified to accept the probe. This door fits many of the viewports at the station. This will allow us to simply

remove the existing door and install the door with the probe already in place; thus providing a better seal.

Final preparations are being made with FirstEnergy personnel for the testing mid-July. Current plans are to arrive and begin testing the week of July 15. It is anticipated that the testing will be completed within a three to five week period.

**Task 3.2 Soot**

During this quarter, progress was made on both computational and experimental tasks.

**Simulation**

Simulations of the L1500 (4.5 mmBTU) pilot scale test furnace at the University of Utah Combustion Research Laboratory have been performed using a soot model originally developed by Fletcher [Fletcher et al, 1992], [Brown & Fletcher, 1998] which has been implemented into REI’s two phase combustion CFD code *GLACIER*. Operating conditions and coal properties (Illinois #5) are shown in the following Table 3.2.1.

Table 3.2.1 Pilot-scale Test Furnace Operating Conditions and Coal Properties

Burner S.R.	0.85	As Received [%]	
Overall S.R.	1.15	C	65.99
Primary air flow rate [LB/HR]	473	H	3.97
Secondary air flow rate [LB/HR]	700	O	8.47
Tertiary air flow rate [LB/HR]	1392	N	1.29
Staging air flow rate [LB/HR]	929	S	3.49
Coal feeding rate [LB/HR]	345	Ash	9.87
Coal firing rate [MMBTU/HR]	4.01	Moisture	6.92
Swirl Number			
Secondary	0.5		
Tertiary	0.5		
Backside wall temperature [K]	350		
Wall emissivity	0.7		
Wall thermal resistance [m2K/W]	0.08		
Inlet temperature (coal and air) [K]	300		

Illustrated in Figure 3.4 are selected simulation results at the center cross-section of the furnace. As shown, there is nearly complete combustion of soot at the location of the staging port due to additional air introduction. Based on the simulation results, it was determined to sample for the soot particles between the burner exit and the staging port at furnace section 3 (3.25 meters from the burner exit).

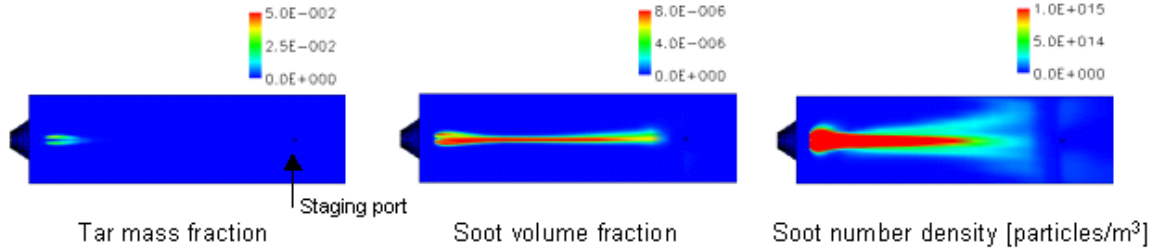


Figure 3.4 Calculated Tar and Soot Levels in Pilot-scale Test Facility

The estimated average soot volume fraction upstream of the staging port in the *GLACIER* simulations is about  $1.6 \times 10^{-7}$ . According to [Veranth, 2000], about 0.2 ~ 0.6% of the fuel carbon forms soot (or small char) for low-NOx burner with bituminous coal. As noted below, the average soot volume fraction just upstream of the staging air is about  $3.2 \times 10^{-7}$

$$f_v = \frac{(345 \text{ lb/hr})(0.4536 \text{ kg/lb})(1/1950 \text{ m}^3/\text{kg})(0.6599)(0.006)}{(473 + 700 + 1392 \text{ lb/hr})(0.4536 \text{ kg/lb})(1/1.177 \text{ m}^3/\text{kg})} = 3.2 \times 10^{-7} \text{ (@} \sim 300\text{K)}$$

which is in agreement with the CFD simulation results.

### Experiment

A pilot-scale test facility (L1500) was operated according to the conditions used in the *GLACIER* simulation. Soot was sampled at various locations along the furnace section using a water-cooled sampling probe. Sampling locations were selected between the burner exit and a staging port at furnace section 3, as simulation results showed very low soot concentration beyond the staging port. Particles larger than 2.5  $\mu\text{m}$  were knocked out by a cyclone before entering a dilution chamber. A photoacoustic analyzer (PA) was used to measure soot concentrations coming out of the dilution chamber. The centerline measurements are shown in Figure 3.5 along with *GLACIER* simulation results.

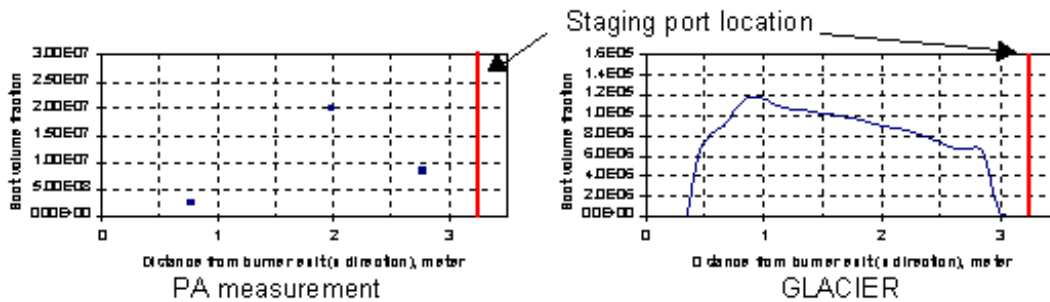


Figure 3.5 Measured and Predicted Soot Concentrations along the Centerline of the Pilot-scale Test Facility

Generally, PA measurements show a similar trend to simulation results along the centerline of the furnace but with much lower concentrations by two orders of magnitude. One of the factors



that may explain this is wall deposition. A water cooled sampling probe was used instead of a transpiration probe because the small cyclone in the sampling system limits the possible sampling flow rate. In addition, a low sampling flow rate will make wall deposition worse.

Figure 3.6 shows the tip of the sampling probe after the experiment. The probe tip was covered with soot-like material as were the inside walls of the probe. This will result in a measurement somewhat lower than the actual concentration. On the other hand, the low sampling flow rate (lower than isokinetic sampling flow rate) will result in an increase in the measured concentration. However, this may not be a significant factor since soot particles are normally small. Particle size from the simulation was less than 1  $\mu\text{m}$ . Wall deposition in the water-cooled probe may be a dominant factor in explaining the lower experimental concentrations in comparison to computational results. The calibration of the PA system is being verified, because it tends to give significantly lower concentrations than observed in the previous pool-fire measurements.



Figure 3.6 Tip of the Sampling Probe after Testing in the Pilot-scale Facility

For the next experiment, a larger cyclone will be used. This will allow for the use of a transpiration probe. In addition, more sampling locations will be selected to more thoroughly evaluate the oxidation feature of the soot model. Additional pilot-scale simulations will be performed as part of this evaluation.

## Task 4 - SCR Catalyst Performance under Biomass Co-Firing

Near the end of this performance period, a contract modification was received from DOE for proposed modifications to our SCR task. The contract modification provides funding to allow including Prof. Larry Baxter (Brigham Young University) in the modified program and will us to evaluate SCR costs at a deeper level, improve estimates of actual costs and investigate the impact of biomass co-firing. The contract modification has been signed by REI and returned to DOE. A sub-contract has been issued to Brigham Young University to support the work to be performed there by Prof. Baxter and his colleagues. A modification for the existing sub-contract with the University of Utah is in progress.

## Task 5 - Fly Ash Management/Disposal

This task deals with the undesirable adsorption of ammonia on fly ash associated with the operation of advanced NO<sub>x</sub> control technologies such as selective catalytic reduction. The task examines the fundamentals of the adsorption process as well as the fundamental process underlying potential techniques for post-combustion removal of adsorbed ammonia. This task is being performed at Brown University under the leadership of Prof. Bob Hurt.

Work this period focused exclusively on Subtask 5.1: *Ammonia Adsorption Mechanisms*. This subtask examines the fundamental mechanism leading to the initial adsorption, and seeks to understand the effect of temperature, ammonia slip level, flue gas composition, and ash type on ammonia contamination levels.

### Task 5.1 Ammonia Adsorption Mechanisms

#### Industry Involvement

On May 23 Brown staff participated via conference call in a meeting of a working group on ammonia, assembled by EPRI at Southern Company facilities in Birmingham, AL. The working group includes engineers from around the country active in various aspects of the ammonia contamination problem. During the meeting contractors exchanged information on their ongoing work ranging from adsorption mechanisms, to analytical techniques and removal processes. The industry participants made suggestions regarding research needs that are not being fulfilled by the current set of experimental programs in the U.S.

#### Analysis of Ammonia Adsorption Isotherms

Work on ammonia adsorption mechanisms began with a custom retrofit of an automated vapor adsorption apparatus and the measurement of complete adsorption isotherms in the pure ammonia system. The analysis of data for a representative class F ash (FA21 from the Brown University sample bank: 6.2% LOI from Brayton Point) was completed this quarter and the most significant results summarized below.

Figure 5.1 shows adsorption data for the fly ash before and after carbon removal by air oxidation. Above  $10^{-4}$  relative pressure the adsorption of ammonia is significant and dominated by carbon rather than the mineral portions of the ash. Below  $10^{-4}$  relative pressure the adsorbed amounts are small for all samples. Note that the relative pressure is defined as  $P/P_0$ , where  $P_0$  is the saturation pressure for ammonia (4.2 bar at 273 K). An important feature is the sharp uptake at around  $10^{-4}$  relative pressure. This feature was reproducible in all of the experiments with the as-received fly ash 21. A similar feature is not visible, at either the same relative pressure or at the same absolute pressure, in the results from nitrogen and carbon dioxide — it is unique to ammonia. Ozonation of the carbon surfaces enhances this feature, while the rest of the isotherm is not significantly altered, suggesting that this feature is related to surface oxides on carbon.

There have been a significant number of studies concerned with the adsorption of ammonia on carbons (e.g. Boehm et al., [1964] and Hofman et al. [1950]). These studies have also shown that oxide groups on the surface of a carbon enhance the adsorption of ammonia. It is often

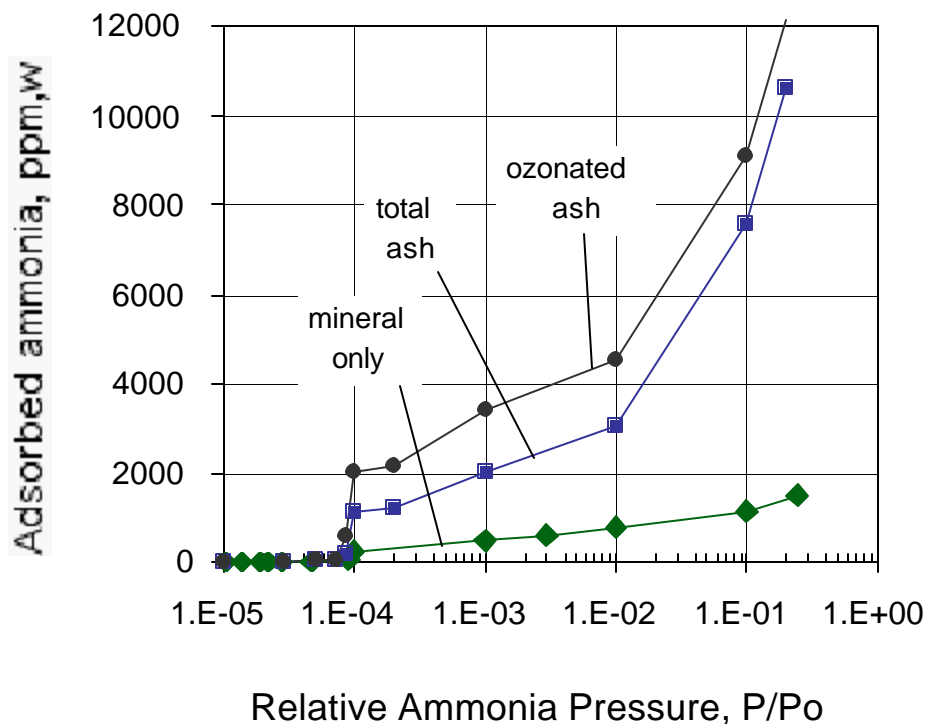


Figure 5.1. Full ammonia adsorption isotherms on A21 fly ash (6.2% LOI from Brayton Pt.) at 273 K before and after carbon removal by air oxidation. Also shown is the ammonia isotherm on fly ash subjected to ozonation.

hypothesized that the acidic functional groups associated with the surface oxides act as Bronstead acids towards ammonia, which is a strong base [Zawadski, 1989]. These acid functionalities donate a proton to the ammonia in an acid-base interaction, yielding an ammonium ion,  $\text{NH}_4^+$ . There is also evidence of formation of groups which cannot be hydrolyzed in acid solution. The suggestion has been made that the ammonia reacts with surface acid groups, probably yielding amides, or possibly even imides. As the temperature of the complexes is raised, the irreversibly formed amide groups can decompose, eventually giving rise to cyano groups on the carbon surface. Hence, the adsorption process involving reaction of ammonia with acid groups to form amides may be observed to be irreversible, even at high temperatures.

The information of most interest with respect to the ammonia slip issue is contained in the region of the isotherm most near the zero relative pressure axis (1-20 ppm). To show the behavior at low pressures more clearly, the isotherms can be expanded on the X-axis and the partial pressure units converted to an equivalent ppm by volume in a 1 atm gas (e.g. flue gas). The results are shown in Figure 5.2. A low-concentration asymptotic value in Figure 5.2 appears to be about 20 ppm and independent of the carbon content. This is comparable to the theoretical amount of ammonia corresponding to one monolayer on the geometric external surface of the mineral grains. In fact analysis of this isotherm yields an ammonia-BET surface area of  $0.7 \text{ m}^2/\text{g}$ , which

is in excellent agreement with the values earlier obtained from nitrogen isotherms for the carbon-free ash. It appears that this monolayer coverage of the mineral grains occurs at very low vapor concentrations, while at higher ammonia concentrations carbon begins to dominate the adsorption process.

Figure 5.3 shows that the adsorbed ammonia amounts are similar to those of  $N_2$  or  $CO_2$  when compared at common values of  $P/P_0$ . This suggests that much of the ammonia adsorption is physical in nature. The effect of ozonation in Figure 5.1 suggests a parallel chemisorption route, so it is likely that both mechanisms contribute to overall ammonia adsorption.

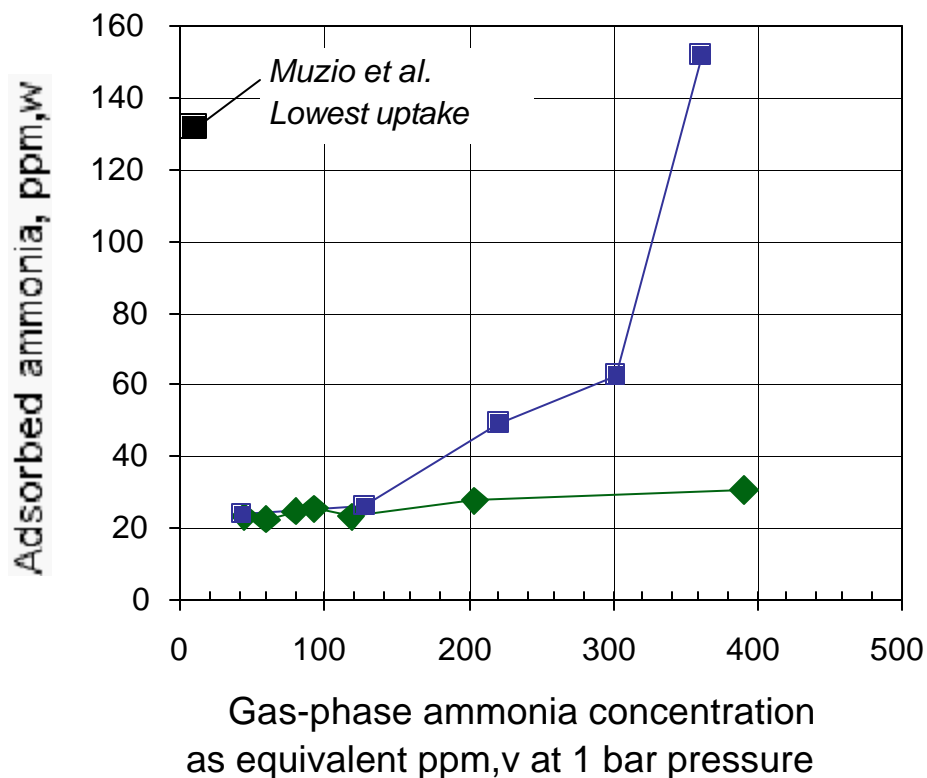


Figure 5.2. Ammonia isotherms from Figure 5.1 with the low partial pressure region expanded and the X-axis units converted to those commonly used to express ammonia slip concentrations.

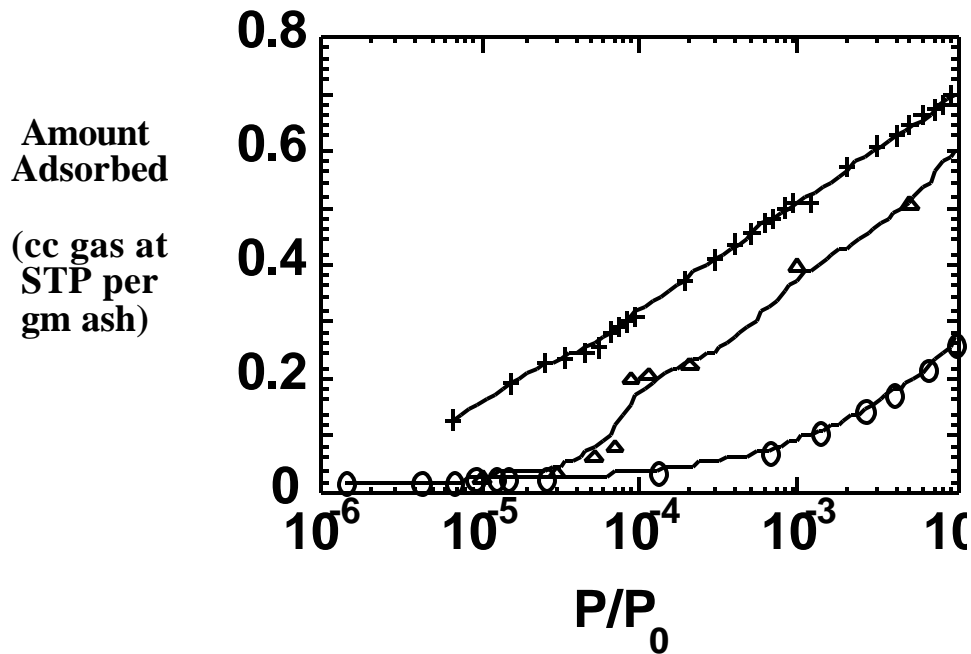


Figure 5.3. Comparison of ammonia, nitrogen, and carbon dioxide adsorption on fly ash 21 over the same range of relative pressure. Crosses: nitrogen; triangles: ammonia; circles: carbon dioxide.

Of particular interest is the comparison between the present results and the experiments of Muzio et al. [1995] in simulated flue gas. Muzio et al. measure 132-347 ppm,w of ammonia adsorbed on a range of ash samples exposed to 10 ppm ammonia slip at 150 °C — the lowest of these data points is shown on Fig. 5.2 for comparison. The low uptake in the present experiments cannot be explained by the low temperature (273 K vs. 423 K in Muzio et al.), as we have observed decreases in uptake with increasing temperature above 273 at constant partial pressure. The difference most likely lies in the secondary gas species as discussed in the section below.

### Continuous Flow Experiments with $\text{SO}_2 / \text{NH}_3$

The data of Muzio et al. [1995] show much higher uptakes of ammonia than in the isotherms presented above (see Fig. 5.2). Resolution of this discrepancy should provide important information on the mechanisms of ammonia adsorption, and will therefore be investigated in detail. Specifically, Muzio et al. measure 132-347 ppm,w of ammonia adsorbed on a range of ash samples exposed to 10 ppm ammonia slip at 150 °C. The synthetic flue gas had the following composition:

$\text{H}_2\text{O}$	8%
$\text{CO}_2$	14%
$\text{O}_2$	3%
$\text{SO}_2$	1500 ppm
$\text{NH}_3$	0-20 ppm

with the balance being nitrogen and temperatures set at 120-160 °C. The SO<sub>2</sub> level was set to be representative of the expected value burning a high sulfur (2-2.5%) coal.

In order to reconcile our data with that of Muzio et al. [1995] one or more of the secondary components of the flue gas (H<sub>2</sub>O, CO<sub>2</sub>, O<sub>2</sub>, SO<sub>2</sub>) must play a synergistic role in ammonia adsorption. It is well known that SO<sub>3</sub> reacts with ammonia to yield a condensed phase product that can corrode air heaters [Afonso et al., 2001], damage SCR catalysts, and become incorporated into the fly ash, typically as ammonium bisulfate, [NH<sub>4</sub>]<sup>+</sup>[HSO<sub>4</sub>]<sup>-</sup>. Less clear is the role of SO<sub>2</sub>, which is much more abundant in the flue gas than SO<sub>3</sub>, but is also less reactive toward ammonia.

During this period, the first continuous flow experiments were carried out to investigate synergistic effects during the co-adsorption of NH<sub>3</sub> and SO<sub>2</sub>. The goal of the first set of experiments was to test the flow system and to determine if SO<sub>2</sub> addition increased the extent of ammonia adsorption with all other experimental variables held constant. A system of two permeation tubes established desired concentrations of NH<sub>3</sub> and SO<sub>2</sub> in separate streams of N<sub>2</sub> carrier gas, which were mixed and passed over a bed of commercial class F fly ash. After preliminary studies indicated the time required for equilibration, a set of experiments was conducted at room temperature using high concentrations to establish the effect (200-1000 ppm NH<sub>3</sub>; 0-1000 ppm SO<sub>2</sub>). Addition of SO<sub>2</sub> was observed to greatly increase the ammonia uptake.

A review of the literature indicates that ammonia is capable of reaction with SO<sub>2</sub> to produce one of a variety of products including ammonium sulfite, bisulfite, sulfate, bisulfate, or under dry or trace water conditions, amidosulfurous acid (NH<sub>3</sub>SO<sub>2</sub>) or ammonium amidosulfite, (NH<sub>3</sub>)<sub>2</sub>SO<sub>2</sub>. These latter compounds are the anhydrous versions of ammonium bisulfite and ammonium sulfite, respectively. However, in the absence of fly ash or other high area substrates, ammonia is observed to react with SO<sub>2</sub> only at temperatures below about 55-75 °C in the presence of water [Hjuler, Dam-Johansen, 1992], or at even lower temperatures under dry or trace water conditions [Bai et al. 1992]. In the presence of water near room temperature, a liquid-like product is first observed, likely ammonium bisulfite, which subsequently oxidizes to the stable solid, ammonium bisulfate [Hjuler, Dam-Johansen, 1992].

Both our data and these previous studies suggest an important role for SO<sub>2</sub> in the ammonia / fly ash system at room temperature, but its role at temperatures during and prior to fly ash capture (> 100 °C) is still not clear. Water can mediate adsorption of ammonia onto acidic ashes, but it likely requires the formation of a liquid film, and its role is therefore unclear at temperatures in excess of 150 °C. A further possibility is the oxidation of a small portion of the SO<sub>2</sub> to SO<sub>3</sub>, perhaps catalyzed by a component in the fly ash, followed by rapid, stoichiometric reaction between ammonia and the SO<sub>3</sub>. NO<sub>2</sub> has been observed to act as a catalyst in this manner.

In the upcoming periods, we will perform a series of flow experiments at elevated temperature (near 150 °C) adding SO<sub>2</sub>, H<sub>2</sub>O, and O<sub>2</sub>, one component at a time, in order to resolve this mechanism and determine which of the secondary gases is responsible to enhancing ammonia uptake. In the next period we will also report on work done on the second task, which focuses on ammonia *removal* rather than adsorption.

## Task 6 – Field Validation of Integrated Systems

### Future Field Tests

The current schedule for demonstration of Rich Reagent Injection in Ameren's Sioux Unit 1 is early September, 2001. Sioux Unit 1 is a 488 MW, ten-barrel cyclone furnace with opposed wall firing. An overfire air system for this unit has been recently installed. However, optimization of the system is not yet complete and may not be finished prior to the RRI demonstration. The injection skids and RRI ports have been constructed and installed. Oceanside Engineering (Irvine, CA) working with the Electric Power Research Institute (EPRI) has constructed and installed the skids.

## Results and Discussion

Previous modeling and field tests conducted as part of this project have demonstrated that Rich Reagent Injection (RRI) can provide a significant NO<sub>x</sub> reduction for cyclone furnaces. A second field test of RRI for a cyclone furnace is scheduled for Fall, 2001 and will hopefully further establish this trend. However, cyclone furnaces are a relatively small part of the inventory of utility boilers in the USA. A much larger impact could be achieved if RRI can be shown to be a viable option for NO<sub>x</sub> reduction in PC fired utility boilers. During this performance period model evaluations were conducted to investigate the NO<sub>x</sub> reduction performance of injection of aqueous urea into the burner zone of a PC wall-fired furnace. In the last quarterly report, a discussion was given of PC furnace calculations involving the injection of aqueous urea into the lower furnace of staged PC furnaces. In those calculations, both wall and in-burner injection strategies were investigated. During this quarter, the strategy of in-burner injection was investigated in greater depth through a single burner model of the process. Both the coupled CFD model predictions and the streamline analyses for in-burner reagent injection, in the particular burner geometry investigated here, indicate that up to 20% NO<sub>x</sub> reduction may be achievable when the burner is staged to a stoichiometric ratio of approximately 0.85. However, these simulations do not account for additional NO<sub>x</sub> reduction that may be achieved by placement of reagent injectors in the walls of the staged lower furnace. Additional modeling of the combination of in-burner and wall injection will be pursued next quarter.

During this performance period, our efforts on evaluating the corrosion probe to monitor waterwall wastage have been divided along two tracks. The first track has been continued efforts to calibrate the probe using bench and pilot scale experiments to compare measured corrosion rates and corrosion rates predicted by the corrosion probe. The second track of effort has focused on implementing design improvements and assembling and validating a second probe for use in field tests that are scheduled for Summer 2001. The first field test is scheduled to start in the mid-July, 2001.

During the last quarter work, implementation of the soot model into our CFD code has been completed and a set of test data was obtained from the University of Utah L1500 pilot scale test facility. Comparisons of predicted and measured values for the soot generation shows the soot model captures the correct qualitative trends but additional work will be required to improve the

quantitative agreement. Further computational and experimental work is planned for next quarter.

Experiments are on-going to study the adsorption of ammonia onto fly ash for a pure ammonia gas stream and for a simulated flue gas that contains sulfur. For pure ammonia, measurements of ammonia vapor adsorption isotherms on fly ash under carefully controlled conditions indicate a small uptake (about 20 ppm) at low gas phase concentrations (<30 ppm) predominately on the external surface of the mineral grains. At higher gas phase concentrations adsorption on carbon dominates, with evidence for both physical adsorption and parallel chemical adsorption on sites associated with carbon surface oxides. In these pure ammonia experiments the adsorbed amounts are smaller than in experiments with simulated flue gas, suggesting that one or more of the secondary species, SO<sub>2</sub>, H<sub>2</sub>O, O<sub>2</sub> are active in enhancing ammonia adsorption. (This enhancement is in addition to the well known reaction between SO<sub>3</sub> and ammonia leading to bisulfate aerosol or deposit.) New flow experiments indicate an enhancing role of SO<sub>2</sub> at room temperature. Experiments are underway at fly ash capture temperatures of 150 °C in which the secondary flue gas species will be introduced to the ammonia stream one at a time or in pair-wise combinations to reveal the nature of the complex adsorption processes. Work is also underway on the fundamentals of post-combustion ammonia removal processes.

## Conclusions

Good progress has been made on several fronts during the last three months. In particular:

- To address the issue of how to use RRI for NO<sub>x</sub> reduction in PC fired furnaces, a single burner modeling study was performed for injecting reagent directly into the burner. Model results indicate that up to 20% NO<sub>x</sub> reduction may be achievable when the burner is staged to a stoichiometric ratio of approximately 0.85. Additional NO<sub>x</sub> reduction might be achieved by layering in-burner injection with wall injection strategies within the furnace.
- Bench and pilot scale tests are being conducted to calibrate a corrosion probe to monitor water wall wastage. Preparations are being made for conducting a field test of the corrosion probe.
- Preliminary comparisons have been completed for predicted model values and experimental data for soot generation in a pilot scale test furnace under low NO<sub>x</sub> firing conditions.
- A first set of fundamental ammonia isotherms was measured on commercial carbon-containing fly ash samples and compared to similar data for nitrogen and carbon dioxide to understand the fundamental nature of ammonia adsorption. The governing mechanism shifts from mineral adsorption to combined physical/chemical adsorption on carbon as the gas phase ammonia concentration increases. Uptake in simulated flue gas is higher than in pure ammonia, likely due to synergistic effects of one of the secondary species, which will be the subject of future experiments.



Plans for the next quarter include: continued RRI modeling to investigate the potential benefit of combining in-burner and wall injection strategies for PC fired utility boilers; completing the calibration tests of the corrosion probe and performing a field test in a utility boiler with the corrosion probe; further improvements to the soot model in our CFD code and pilot scale tests to collect data on soot generation for use in verifying the soot model; commence work on our SCR catalyst task; and continued studies on ammonia adsorption onto fly ash and possible removal processes.

## Literature References

Afonso, R., Tavoulares, S., Stallings, J., "Prediction and Mitigation of Air Preheater Fouling due to Ammonium Bisulfate," *Sixth International Conference on Technologies and Combustion for a Clean Environment*, Oporto, p.1519 (2001)

Bai H., Biswas, P., Keener, T.C., *Ind. Eng. Chem. Res.* 31 88-94 (1992).

Boehm, H.P., Diehl, E., Heck, W., and Sappok, *Angew. Chem.* 76, 742 (1964).

Brown, A.L., Fletcher, T.H., *Energy Fuels*, 1998, Vol 12, pp. 745-757.

Fletcher, T.H., Kerstein, A.R., Pugmire, R.J., Solum, M.S. and Grant, D.M., *Energy Fuels*, 1992, vol. 6, pp. 414-431.

Hjuler, K., Dam-Johansen, K., *Ind. Eng. Chem. Res.* 31 2110-2118 (1992).

Hofman, U. and Ohlerich, G. *Angew. Chem.* 62, 16 (1950).

Muzio L.J., Kim, E.N., McVickar, M., Qartucy, G.C., McElroy, M., Winegar, P., "Ammonia Absorption on Coal and Oil Fly Ashes," *Joint EPRI/EPA Symposium on Stationary Combustion NOx Control*, Kansas City, 1995.

Veranth, J., *Fuel*, **79**, pp.1067-1075, 2000.

Zawadzki, J. *Chem. and Phys. Carbon*, 21, p147, Dekker, New York (1989).